Available online at www.sciencedirect.com
SCIENCE DIRECT
Journal of Electroanalytical Chemistry 589 (2006) 195–202
Journal of Electroanalytical Chemistry
www.elsevier.com/locate/jelechem

Deposition of HgTe by electrochemical atomic layer epitaxy (EC-ALE)

Venkatram Venkatasamy [a], Nagarajan Jayaraju [a], Stephen M. Cox [b], Chandru Thambidurai [a], Mkhulu Mathe [a], John L. Stickney [a,*]

[a] Department of Chemistry, University of Georgia, 1001, Cedar Street, Athens, GA 30602, United States
[b] Department of Astronomy and Physics, Athens, GA, United States

Received 17 November 2005; received in revised form 27 January 2006; accepted 9 February 2006
Available online 4 April 2006

Abstract

This paper describes the first instance of HgTe growth by electrochemical atomic layer epitaxy (EC-ALE). EC-ALE is the electrochemical analog of atomic layer epitaxy (ALE) and atomic layer deposition (ALD), all of which are based on the growth of materials a monolayer at a time, using surface limited reactions. EC-ALE involves the successive application of electrochemical surface limited reactions such as underpotential deposition (UPD), to form the desired material in a series of steps, a cycle, to produce a monolayer of the material. The number such cycles then determines the thickness of the resulting deposit. This study describes attempts to optimize an EC-ALE cycle for the growth of HgTe. The effect of changes in the deposition potentials for Hg and Te are studied, as well as that used to strip excess Te. All depositions took place in an automated electrochemical flow cell deposition system, so that potentials and solutions could be repeatedly changed on the fly. Based on these studies, the best deposits were formed using Hg and Te deposition potentials of 0.40 V and −0.35 V, respectively, and using a Te stripping potential of −0.70 V. Ellipsometric measurements of 100 cycle deposits formed using these conditions showed a film thickness of 71.9 nm, about twice that expected, based on the view that each cycle should result in one HgTe compound monolayer. Electron probe microanalysis (EPMA) of the deposit indicated a Te/Hg atomic ratio of 1.02, the expected stoichiometry for the deposit. Electrochemical quartz crystal microbalance (EQCM) studies of this cycle, also using an automated flow cell, indicated that some deposited Te was stripped at the potential used to deposit Hg. X-ray diffraction studies showed the deposits to grow in a strongly (1 1 1) orientation. Room temperature IR absorption studies of HgTe indicated a negative bandgap, −0.20 eV.

Keywords: HgTe; EC-ALE; EQCM; EPMA; Ellipsometry; IR detectors; XRD

1. Introduction

Mercury telluride, HgTe, is a II–VI compound, which has gained importance for its use in the development of Mer Cad Tel ($Hg_{(1-x)}Cd_xTe$) IR detector material [1–5]. HgTe is a semi metal with a negative band gap, −0.14 eV at 300 K [6]. Incorporation of Cd into this matrix results in a bandgap anywhere between −0.15 and 1.6 eV, bandgap engineering, making it a very desirable detector material. HgTe has been formed by ALE [7], flash evaporation [8] and electrodeposition [34]. Seyam and Elfalaky synthesized *p*-type HgTe with a bandgap between 0.02 and 0.3 eV [8]. Optical properties of HgTe, formed by MBE, have been the subject of several papers [9,10].

Electrochemical atomic layer epitaxy (EC-ALE) is the electrochemical analog of atomic layer epitaxy (ALE) [11–13] and atomic layer deposition (ALD) [14–17], both of which are gas or vacuum phase thin film formation techniques based on deposition one atomic layer at a time, using surface limited reactions. Underpotential deposition (UPD), is used in EC-ALE to achieve atomic layer by atomic layer growth [18–22]. UPD is the deposition of one element on a second at a potential prior to that needed to deposit the element on itself, the result of the free energy of compound formation between the depositing element and the terminating element of the deposit surface.

* Corresponding author. Tel.: +1 706 542 2726; fax: +1 706 542 9454.
E-mail address: stickney@chem.uga.edu (J.L. Stickney).

0022-0728/$ - see front matter © 2006 Elsevier B.V. All rights reserved.
doi:10.1016/j.jelechem.2006.02.006

A number of II–VI [23–25] and III–V [26–28] compound semiconductors have been successfully deposited by EC-ALE. The use of separately optimized precursor solutions for each of the depositing elements, as well as separate deposition potentials, times, etc., has proven to be very important for the successful deposition of a wide variety of materials. EC-ALE has recently been applied to the deposition of metals, layer by layer, using redox replacement of an atomic (UPD) layer of a more reactive metal by a more noble metal.

This paper is the first report of the deposition of HgTe by EC-ALE. All depositions were performed in an automated flow deposition system [29–31]. The dependence of the HgTe deposit structure and composition on the potentials for Hg and Te, as well as the Te reductive stripping potential, was investigated. Studies were performed using ellipsometry, optical microscopy, X-ray diffraction (XRD), electron probe micro analysis (EPMA) and Fourier transform infrared spectroscopy (FT–IR). Optimal conditions obtained were further studied using an electrochemical quartz crystal microbalance (EQCM) flow cell to better understand the deposition process.

2. Experimental

The electrochemical flow deposition system used for these studies has been previously described [29–31]. Pump heads, valves and tubing were confined inside a nitrogen purged Plexiglas box to limit oxygen, which affects deposit quality. The electrochemical cell consists of a thin-layer design to promote laminar flow. The auxiliary electrode was an ITO glass slide (Delta Technologies Ltd., Stillwater, MN), and the reference electrode was Ag/AgCl (3 M NaCl) (Bioanalytical Systems Inc., West Lafayette, IN). Substrates consisted of 300 nm thick gold films on glass. The substrates were annealed at 400 °C for 12 h under a vacuum of 10^{-6} Torr, after Au vapor deposition, resulting in a (1 1 1) habit. The working and auxiliary electrodes were held apart by a 2 mm thick silicon rubber gasket, which defined a $1 \times 3\ cm^2$ rectangular opening where deposition took place. The ITO auxiliary was transparent, allowing deposition to be followed visually. The reference electrode, Ag/AgCl (3 M NaCl) was positioned at the cavity outlet.

The solutions used were 0.2 mM HgO, pH 2 and 0.2 mM TeO_2, pH 4, and both contained 0.5 M Na_2SO_4. The blank solution contained only the 0.5 M Na_2SO_4, at pH 4. Solution pH was adjusted using H_2SO_4. Water used for solutions was supplied from a Nanopure water filtration system (Barnstead, Dubuque, IA) attached to the house DI water system. Chemicals were reagent grade or better.

The basic EC-ALE cycle used to deposit HgTe was as follows: the Te solution was flushed into the cell for 2 s (40 mL/min), and held quiescent for 15 s, all at the potential chosen for Te deposition. Blank solution was then flushed through the cell for 3 s. This was followed by filling the cell with the Hg solution for 2 s, and holding quiescent for 15 s for deposition. The cycle was then completed by flushing with blank for 3 s. For the majority of the deposits discussed here, this cycle was repeated 100 times.

Deposit thickness was monitored using a single wavelength ellipsometer (Sentech SE 400). A Scintag PAD-V diffractometer with Cu Kα radiation ($\lambda = 1.5418$ A), was used to obtain glancing angle X-ray diffraction patterns. Electron probe microanalysis (EPMA) was run on a Joel 8600 wavelength dispersive scanning electron microprobe. Glancing angle absorption measurements were performed, using an FT–IR spectrophotometer (Bruker FTS-66v, Bruker optics Inc.).

Optimal deposition conditions were studied using a flow cell based electrochemical quartz crystal microbalance (EQCM). A 9 MHz AT-cut quartz crystal (Seiko EG&G) was used, where both sides were coated with circular Au electrodes (ca. 0.2 cm^2, 5 mm in diameter). The electrodes were formed with 50 nm of Ti, followed by 300 nm of sputtered Au. Calibration of the EQCM was carried out using Ag electrodeposition coulometry.

3. Results and discussion

The deposition potentials initially chosen for Hg and Te, and used in the first EC-ALE cycle, were obtained from cyclic voltammetric data for Au electrodes in the Hg and Te solutions. The use of upd potentials obtained from cyclic voltammetry on Au must be considered a first approximation, as the potential needed to form atomic layer on the growing deposit generally differ from those on the substrate. However, values for UPD on Au provide a set of potentials for an initial cycle.

The voltammetric behavior of Hg^{2+} on gold on glass electrodes is shown in Fig. 1. The Hg scan was started at 0.95 V in the cathodic direction. Two distinct reduction peaks were observed at potentials of 0.45 and 0.30 V. These correspond to upd and bulk reduction features of Hg^{2+}, respectively. Corresponding stripping features for bulk and UPD Hg occurred at 0.42 and 0.55 V, respectively (dotted curve in Fig. 1). It is interesting to note, that as the potential was scanned negative of 0.30 V, no further increase in the bulk Hg oxidation feature (0.42 V) was observed. However, a new peak between 0.70 and 0.75 V did appear, and grew as the negative limit for the scan decreased. It is well known that Hg forms amalgams with Au, and present results (Fig. 1) suggest that most of the additional Hg, deposited below 0.30 V, went subsurface, forming a surface amalgam. Stripping this surface amalgam then required a more positive potential than that for Hg UPD stripping, accounting for the most positive oxidation peak and its growth.

The voltammetry of a gold on glass substrate in the 0.2 mM $HTeO_2^+$, pH 4, solution is shown in Fig. 2. The cathodic Te scan was started at 0.95 V and displayed $HTeO_2^+$ reduction peaks at −0.35, −0.10 and 0.28 V, corresponding to the bulk, upd (I) and upd (II) peaks, respectively. Further scanning in the cathodic direction resulted

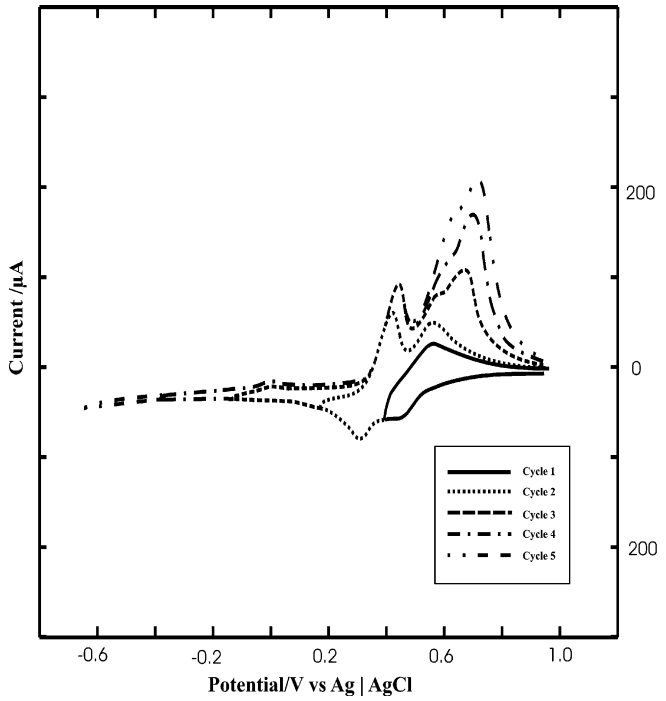

Fig. 1. Cyclic voltammogram of Au electrode in 0.5 mM Hg^{2+}, pH 2 (electrode area: 4 cm^2, scan rate: 5 mV/s).

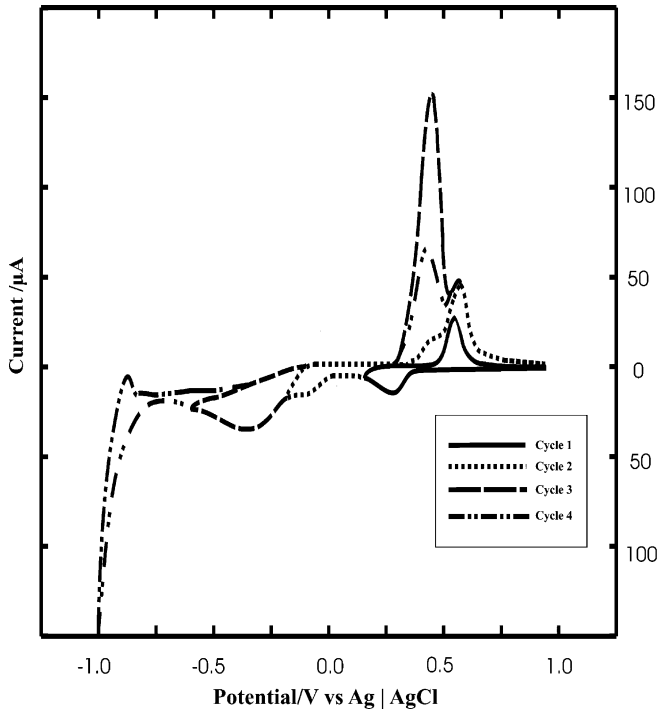

Fig. 2. Cyclic voltammogram of Au electrode in 0.2 mM $HTeO_2^+$, pH 4 (electrode area: 4 cm^2, scan rate: 5 mV/s).

in hydrogen evolution below −0.80 V, as well as the reduction of some bulk Te to a telluride species such as HTe^-. During subsequent anodic scans, peaks at −0.75, 0.42 and 0.55 V were evident, which correspond, respectively, to HTe^- oxidation, bulk and upd stripping.

The preliminary EC-ALE cycle, designed to deposit HgTe, was constructed as follows: the Te solution was rinsed into the cell for 2 s at 0.20 V, at which point the solution was held without flowing, quiescent, for 15 s to deposit the Te atomic layer. In order to avoid co-deposition of HgTe by mixing Hg^{2+} and $HTeO_2^+$ ions in the cell, a blank rinse step, at 0.20 V, was used to flush the Te solution before introduction of the Hg solution. This was followed by a 2 s rinse with the Hg solution and 15 s quiescent deposition at 0.48 V. The cycle was completed by rinsing again with the blank solution, to conclude one EC-ALE cycle. In general, in this study, deposits were formed using 100 cycles.

The above cycle, however, resulted in no observable deposit. From plots of the current vs. time during the 100 cycles, a lack of Te deposited was evident, which is understandable given the slow kinetics for Te deposition, evident by the overpotential needed to deposit Te (Fig. 3) [32]. If an overpotential was used for Te deposition, the Te formed usually consisted of both bulk and UPD components, resulting in more Te than desired. The problems associated with deposition of both bulk and UPD can be minimized by using a short deposition time, as the surface limited reaction (UPD) is significantly faster than bulk deposition, and bulk deposition must, by definition, commence only on top of UPD. In the present study after the first deposits did not work, the deposition potential and time were optimized to achieve Te deposition and minimize bulk Te formation. However, some bulk Te was still present, motivating the inclusion of an extra step in which excess, or bulk, Te was reductively stripped at a more negative potential in a blank solution, leaving only an atomic layer of Te [32].

Changes to the existing EC-ALE cycle involved use of a more negative Te deposition potential, and use of the above mentioned Te stripping step to remove any bulk Te remaining. The stripping step involved rinsing the deposit at −0.70 V for 3 s in the blank solution, after the Te deposition step. Bulk Te was reduced to HTe^-, a soluble species that was rinsed away with the blank.

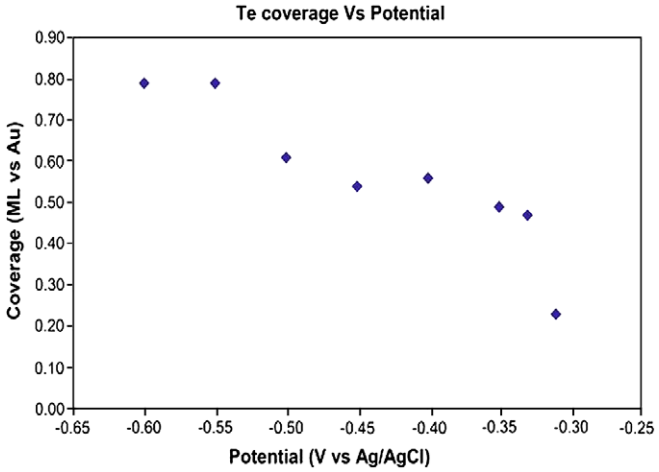

Fig. 3. Effect of Te deposition potential on 100 cycle deposits (Hg deposition potential: 0.40 V; Te stripping potential: −0.70 V).

To optimize the deposition of Te, a series of experiments were performed where the deposition potential of Te was varied from −0.25 to −0.60 V while maintaining the deposition potential for Hg at 0.40 V and the Te stripping potential at −0.70 V. The resulting deposits were analyzed by coulometry, optical microscopy and EPMA. The coulomteric results (Fig. 3) indicated that the deposition of Te did not start until a potential of −0.30 V was used, which again points out the slow kinetics for Te deposition (0.6 V negative of the formal potential for $HTeO_2^+$ reduction). The graph shows a plateau region between −0.35 and −0.55 V, where the ML coverage for Te deposition was nearly constant while the potential was shifted negative. A monolayer (ML) is a unit of coverage defined in surface science as one adsorbate atom for every surface atom. Annealed gold on glass was used as substrate, which generally shows a strongly preferred (1 1 1) oriented growth habit. Thus for the present study, a monolayer was defined assuming the surface to be (1 1 1), with a roughness factor of 1. The actual surface will not be completely (1 1 1) or atomically flat, however, the errors associated with these factors are in opposite directions, minimizing problems. Based on EPMA, optical microscopy and coulometry, −0.35 V was chosen as the best deposition potential for Te.

A similar approach was taken for finding the best Te stripping potential. So the Hg and Te deposition potentials were maintained at 0.40 and −0.35 V, respectively, and the Te stripping potential was varied from −0.35 to −0.95 V. As the deposit thickness was an indirect measure of the amount of Te deposited, and thus an indication of the amount of Te being stripped, the resulting deposits were analyzed by a single wavelength ellipsometer to follow the effect of the stripping step. EPMA and optical microscopy were also performed to determine deposit stoichiometry and morphology, respectively. Fig. 4 shows the dependence of deposit thickness on the Te stripping potential. At the more negative potentials, such as −0.95 V, essentially no deposit was observed, as all the Te (including UPD Te) was stripped. Correspondingly, potentials positive of the telluride reduction potential had little effect on the deposit thickness. Based on optical microscopy and EPMA data for the deposit stoichiometry, −0.70 V was chosen as the stripping potential, even though the deposit thickness was considerably higher than the ideal deposit thickness (71.9 vs. 37.4 nm). The optimal thickness for a 100 cycle deposit is based on the assumption of one Hg–Te bilayer growing each cycle with the (1 1 1) orientation of a zinc blende crystal structure, which should be 37.4 nm.

A possible reason for the excess thickness could be the redox replacement of the deposited Te by Hg ions. It is well known that more active species are oxidized by and exchanged for more noble species, in a redox replacement reaction. Since Hg is nobler than Te, it is possible that some Te was exchanged for Hg. The extra Hg would then react with more Te. Another possibility is that the extra thickness is inherent in the growth of HgTe, and the simple model of one Hg–Te bilayer is faulty. To address this question, an electrochemical quartz crystal microbalance (EQCM) flow cell system was used, and the results will be discussed below.

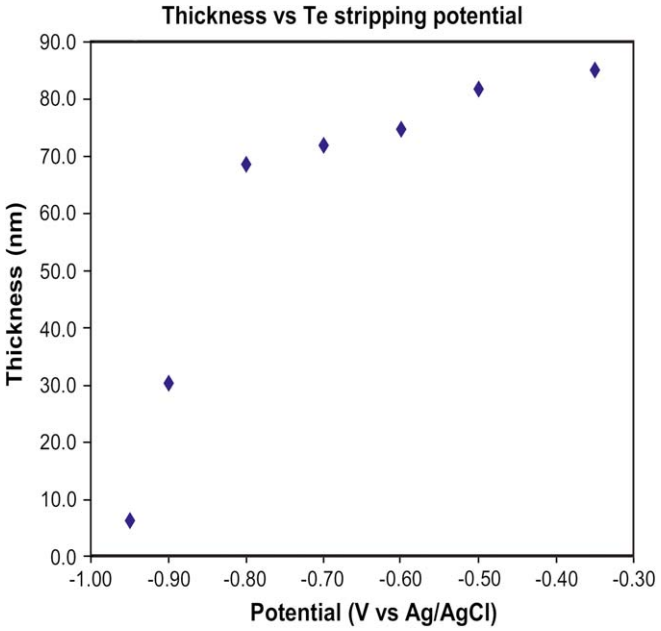

Fig. 4. Effect of Te stripping potential on the thickness of 100 cycle deposits (Hg deposition potential: 0.40 V; Te deposition potential: −0.35 V).

To obtain the ideal deposition potential for Hg, a potential dependence study was performed by keeping the Te deposition and stripping potentials constant at −0.35 and −0.70 V, respectively (Fig. 5). The nature of the deposition of Hg is intriguing, as a typical S shaped curve is evident in Fig. 5. The figure is based on coulometry for the deposition of Hg, as a function of the potential used for Hg deposition. What is intriguing is that at more positive potentials, oxidative currents were observed, not reductions. The negative coverages observed for Hg could probably be due to the simultaneous oxidation of Te at Hg deposition potentials. Further discussions on this topic are given below.

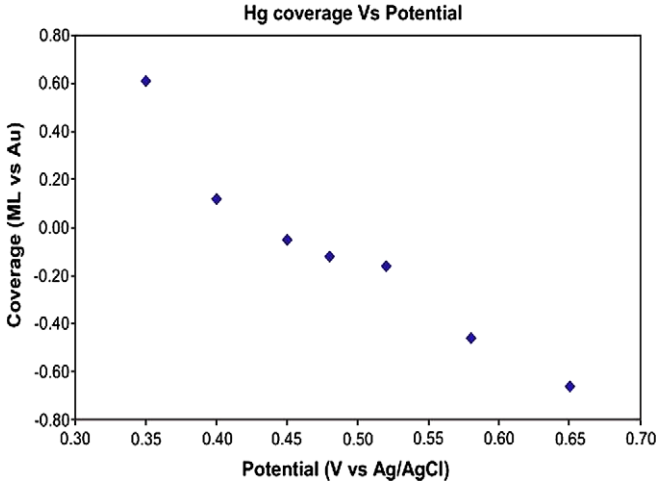

Fig. 5. Effect of Hg deposition potential on 100 cycle deposits (Te deposition potential: −0.35 V; Te stripping potential: −0.70 V).

There is a plateau in the graph, between 0.40 and 0.52 V, but the coverage relating to the plateau corresponds to a coverage of essentially 0 ML. However, based on EPMA results and optical microscopy observations of the deposits, 0.40 V was chosen for Hg deposition.

The following EC-ALE cycle was then chosen (Fig. 6) based on the above mentioned studies: Te solution was rinsed into the cell for 2 s at −0.35 V, and the solution then held static for 15 s, for deposition. The cell was then flushed with blank solution for 3 s at −0.35 V, at which point, the potential was then changed to −0.70 V for 3 s. After which, Hg solution was flushed through the cell for 2 s, and held static for 15 s at 0.40, to deposit. This was followed by another blank rinse at 0.40 V for 3 s.

As noted above, questions concerning this cycle and the deposition mechanism were investigated using an EQCM (electrochemical quartz crystal microbalance) flow cell. Some aspects of the deposition process in the EQCM flow cell differed from those in the standard flow cell hardware used for the majority of the studies here. For instance, experience showed that the EQCM flow cell worked best if solution was continuously flowed through the cell, no static deposition was used, however a much lower flow rate was used (6 mL/min). Overall, use of continuous flow in the EQCM did not appear to significantly change the resulting deposit. The optimal EC-ALE program was repeated for 5 cycles, with the fifth cycle shown in Fig. 7. The cycle to cycle variations were minimal and predictable, allowing conclusions to be drawn concerning the changes in mass between cycles. However, within a cycle, variations in frequency were function of a number of variables besides the masses of electrodeposited atomic layers. For instance, reversibly adsorbed electrolyte may increase, upon adsorption, or decrease, upon desorption, the observed mass changes in a given solution. This forces statements concerning mass changes observed within a cycle to be educated guesses. On the other hand, mass changes from the same points in one cycle to the next are an accurate measure of the mass change for a cycle.

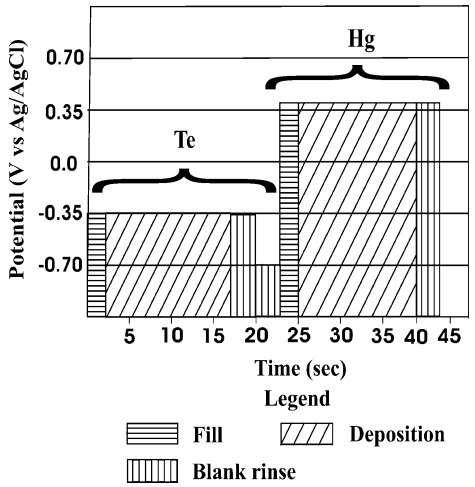

Fig. 6. Optimal deposition program for HgTe deposition.

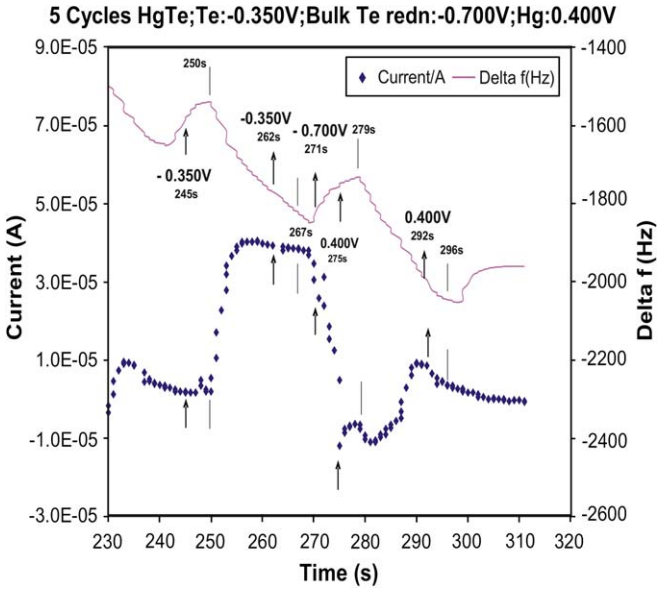

Fig. 7. Current–time profile during HgTe deposition using optimal deposition program by EQCM (5th cycle).

The results shown in Fig. 7 indicate a Te coverage of 2.62 ML from mass and 1.79 ML from coulometry. The Hg coverage was 2.18 ML and −0.39 ML from mass and charge, respectively. The negative Hg coverage, based on charge (Fig. 5), indicates that a net oxidative charge was passed during Hg deposition. The question is then what is being oxidized if Hg^{2+} ions are being reduced? Given the voltammetry for Te (Fig. 2), it is clear that Te may be vulnerable to oxidation at such a positive potential. This then leads to the question of a redox replacement reaction, where deposited Te is traded for Hg at this potential. An experiment devised to investigate this question involved first deposition of three cycles of HgTe, followed by a blank rinse for 17 s at the Hg deposition potential (0.40 V). An oxidation current was observed (Fig. 8), which appears to indicate that Te was being oxidized in the absences of Hg^{2+} ions, as there was nothing else in the solution to oxidize. It was also important to determine the length of time required to oxidize all of the excess Te at Hg deposition potential. So, again the same experiment was performed, but instead of flowing blank for 17 s, a 10 min rinse was performed (Fig. 9), which suggests that it takes about 3 min to strip excess Te from the deposit surface. The net Te coverage was 0.42 ML, on top of the previously deposited Hg layer, very close to the ideal Te coverage of 0.44 ML. From previous studies on CdSe it was found that the formation of one CdSe bi-layer from the (1 1 1) plane of zinc blende CdSe would require 0.44 ML of Cd and 0.44 ML of Se [33]. This is a good approximation of the CdTe, and HgTe in the present case.

The next question is whether Hg^{2+} was replacing Te by a redox replacement reaction. In order to study this problem, three cycles of HgTe were deposited using the deposition program, followed by rinsing with the Hg^{2+} solution for 1 min at open circuit (Fig. 10). The mass of the electrode

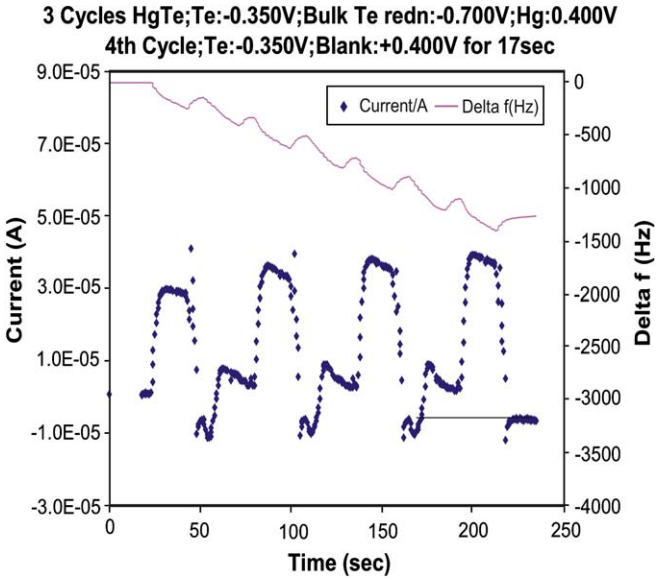

Fig. 8. EQCM experiment showing oxidation of Te at Hg deposition potential (0.40 V).

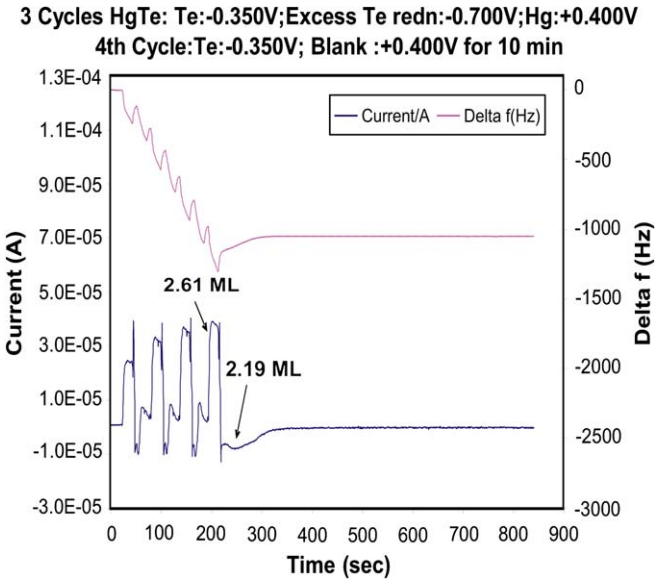

Fig. 9. EQCM experiment showing the time dependence of Te oxidation at Hg deposition potential (0.40 V).

appeared to have increased but not enough to suggest a redox replacement of Te taking place. If there was an actual replacement taking place then the deposited Te would be oxidizing into $HTeO_2^+$, giving out four electrons to Hg^{2+} ions to deposit. So for every Te atom being oxidized, two Hg atoms would be reducing. The mass change in terms of frequency change of the quartz crystal for this reaction would be around 537.8 Hz. This kind of mass change was not observed by the EQCM experiment (137.0 Hz). Moreover, a 3 s blank rinse after the open circuit Hg solution rinse resulted in a corresponding decrease in electrode mass, suggesting desorption of adsorbed Hg ions. These results suggest that Te was not replaced by Hg at open circuit.

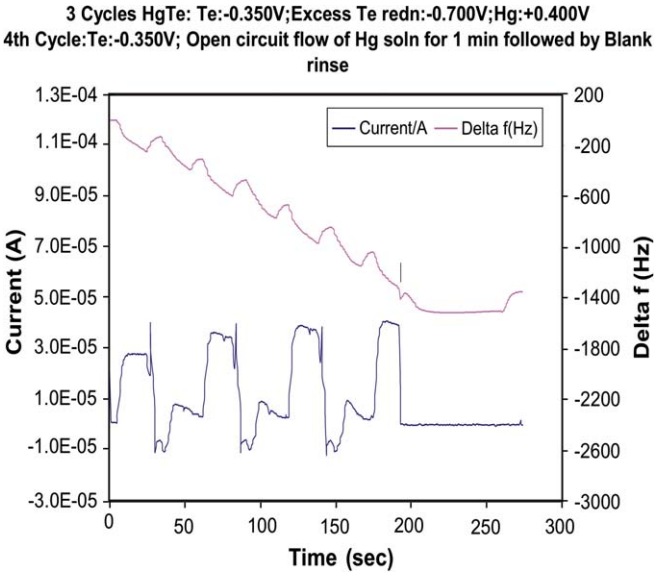

Fig. 10. EQCM experiment to determine redox exchange of Te with Hg at open circuit.

Presently, it is proposed that as Hg is electrochemically reduced on the excess of Te, some Te is simultaneously oxidized. The net current, essentially zero, is thus the sum of that for the reduction of Hg^{2+} ions and for the oxidation of excess Te. Given the above results with the EQCM, where no net replacement of Te was observed at open circuit in the presences of the Hg^{2+} ions, it appears that the deposition of Hg catalyzes the oxidation of Te. If it is assumed that Hg is mobile, and will penetrate into the Te layer, extending the HgTe crystal, this should change the

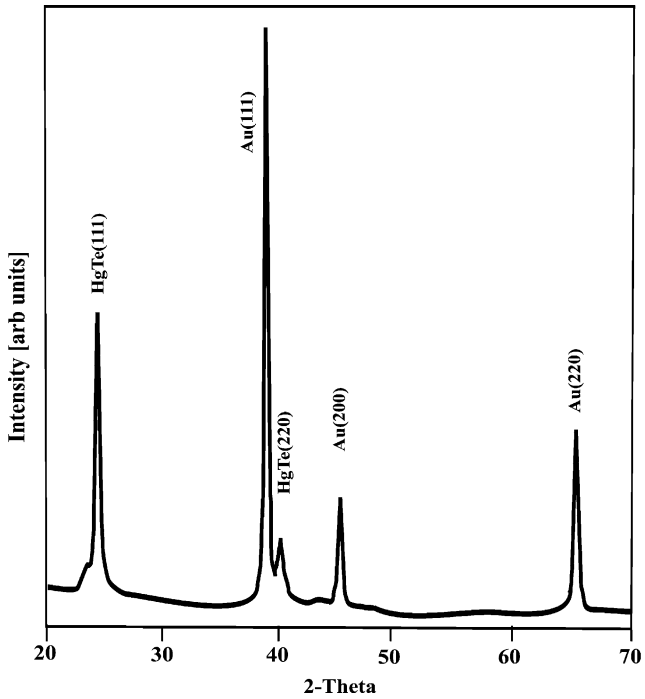

Fig. 11. XRD diffraction pattern of 100 cycle HgTe thin film.

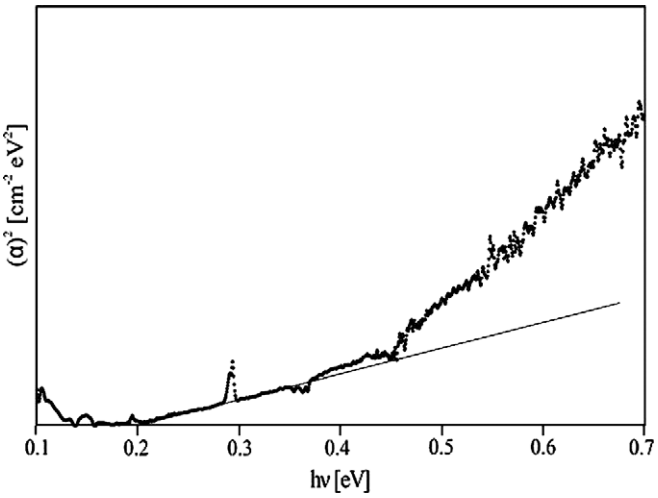

Fig. 12. IR absorption spectrum of 100 cycle HgTe thin film.

bonding of the adjacent layer of Te, possibly making it more reactive, and promoting its oxidation.

Ellipsometric measurements of 100 cycle deposits formed using this program indicate that the film was 71.9 nm thick. EPMA of the deposit indicated a Te/Hg atomic ratio of 1.02. Fig. 11, shows the X-ray diffraction pattern for the deposit. Peaks corresponding to (1 1 1), (2 2 0) and (3 1 1) planes of HgTe (JCPDS 8-469) were evident, and no elemental peaks for Hg and Te were observed. The deposit, however, showed a strongly predominant (1 1 1) orientation. Room temperature IR absorption studies of HgTe were performed using a glancing angle of 85° from the surface normal. Fig. 12 displays a plot of the square of the absorption data vs. energy for the 100 cycle HgTe deposit. An absorption edge was found around −0.20 eV. Much like HgSe, HgTe is also a semimetal, with a negative energy gap. Theoretically, the value of the fundamental energy gap for HgTe is −0.14 eV at 300 K [6].

4. Conclusion

The dependence of nanofilms of HgTe grown using EC-ALE on the deposition potentials used for Hg and Te, as well as that used for a reductive Te stripping step, has been reported. The optimal deposition cycle devised included deposition of Hg at 0.40 V, deposition of Te at −0.35 V and, stripping of excess Te at −0.70 V. The resulting 100 cycle deposit was 71.9 nm thick, more than that expected from the ideal model of one compound monolayer for each cycle, but the deposit was stoichiometric, and showed a strong preferential (1 1 1) orientation. The absorption spectrum for this deposit suggested a negative band gap of 0.20 eV, consistent with the literature. Studies using an EQCM flow cell helped in understanding the deposition process. It was observed that some of the Te each cycle was oxidatively stripped upon switching the potential from the Te deposition potential of −0.35 V to that for Hg deposition, 0.40 V. In addition, it also appeared that Te was not exchanged for Hg. However, the net result was a high quality nanodeposit of stoichiometric HgTe.

Acknowledgments

The authors acknowledge the support of NSF divisions of Material Science and Chemistry.

References

[1] S.R. Hetzler, J.P. Baukus, A.T. Hunter, J.P. Faurie, P.P. Chow, T.C. McGill, Appl. Phys. Lett. 47 (1985) 260.
[2] Y. Guldner, G. Bastard, J.P. Vieren, M. Voos, J.P. Faurie, A. Million, Phys. Rev. Lett. 51 (1983) 907.
[3] J.R. Meyer, A.R. Reisinger, K.A. Harris, R.W. Yanka, L.M. Mohnkern, L.R. Ram-Mohan, J. Cryst. Growth 138 (1994) 981–987.
[4] J.N. Schulman, J. Cryst. Growth 86 (1990) 25–27.
[5] M. Voos, Surf. Sci. Rep. 7 (1987) 189–209.
[6] G.L. Hansen, J.L. Schmit, J. Appl. Phys. 54 (1983).
[7] N.H. Karam, R.G. Wolfson, I.B. Bhat, H. Ehsani, S.K. Ghandhi, Thin Solid Films 225 (1993) 261.
[8] M.A.M. Seyam, A. Elfalaky, Vacuum 57 (2000) 31–41.
[9] C. Janowitz, N. Orlowski, R. Manzke, Z. Golacki, J. Alloy. Compd. 328 (2001) 84–89.
[10] M. Banouni, M. Nasser, G. Leveque, J. Cryst. Growth 159 (1996) 736–740.
[11] S. Bedair, J. Min. Met. Mat. Soc. 45 (1993) 46–50.
[12] T.F. Kuech, P.D. Dapkus, Y. Aoyagi, Atomic Layer Growth and Processing, Materials Research Society, Pittsburgh, 1991.
[13] C.H.L. Goodman, M.V. Pessa, J. Appl. Phys. 60 (1986) R65.
[14] E.B. Yousfi, B. Weinberger, F. Donsanti, P. Cowache, D. Lincot, Thin Solid Films 387 (2001) 29–32.
[15] V. Sammelselg, A. Rosental, A. Tarre, L. Niinisto, K. Heiskanen, K. Ilmonen, L.-S. Johansson, T. Uustare, Appl. Surf. Sci. 134 (1998) 78–86.
[16] M. Ylilammi, Thin Solid Films 279 (1996) 124–130.
[17] M. Leskela, M. Ritala, Thin Solid Films 409 (2002) 138–146.
[18] D.M. Kolb, M. Przasnyski, H. Gerisher, J. Electroanal. Chem. 54 (1974) 25–38.
[19] D.M. KolbAdvances in Electrochemistry and Electrochemical Engineering, vol. 11, Wiley, New York, 1978, p. 125.
[20] K. Juttner, W.J. Lorenz, Z. Phys. Chem. N.F. 122 (1980) 163.
[21] A.T. Hubbard, V.K.F. Chia, D.G. Frank, J.Y. Katekaru, S.D. Rosasco, G.N. Salaita, B.C. Schardt, D. Song, M.P. Soriaga, D.A. Stern, J.L. Stickney, J.H. White, K.L. Vieira, A. Wieckowski, D.C. Zapien, in: New Dimensions in Chemical Analysis, Texas A&M University Press, College Station, TX, 1985, p. 135.
[22] A.A. Gewirth, B.K. Niece, Chem. Rev. 97 (1997) 1129–1162.
[23] L.P. Colletti, J.L. Stickney, J. Electrochem. Soc. 145 (1998) 3594.
[24] B.H. Flowers Jr., T.L. Wade, J.W. Garvey, M. Lay, U. Happek, J.L. Stickney, J. Electroanal. Chem. 524–525 (2002) 273–285.
[25] T.L. Wade, B.H. Flowers Jr., U. Happek, J.L. Stickney, National Meeting of the Electrochemical Society, Spring, Seattle, Washington, 1999.
[26] T.L. Wade, L.C. Ward, C.B. Maddox, U. Happek, J.L. Stickney, Electrochem. Sol. State Lett. 2 (1999) 616.
[27] T.L. Wade, B.H. Flowers Jr., R. Vaidyanathan, K. Mathe, C.B. Maddox, U. Happek, J.L. Stickney, Electrochemical Atomic Layer Eptitaxy: Electrodeposition of III–V and II–VI Compounds, presented at the Materials Research Society, 2000.
[28] T.L. Wade, R. Vaidyanathan, U. Happek, J.L. Stickney, J. Electroanal. Chem. 500 (2001) 322–332.
[29] J.L. StickneyElectroanalytical Chemistry, vol. 21, Marcel Dekker, New York, 1999, pp. 75–211.

[30] T.L. Wade, T. Sorenson, J.L. Stickney, in: Interfacial Electrochemistry, Marcel Dekker, New York, 1999, pp. 757–768.
[31] T.L. Wade, B.H. Flowers Jr., K. Varazo, M. Lay, U. Happek, J.L. Stickney, presented at the Electrochemical Society National Meeting, Washington, DC, 2001.
[32] L.P. Colletti, B.H. Flowers, J.L. Stickney, J. Electrochem. Soc. (1997).
[33] T.E. Lister, J.L. Stickney, Appl. Surf. Sci. 107 (1996) 153.
[34] S. Rath, G.B.N. Chainy, S. Nozaki, S.N. Sahu, Phys. E – Low Dimens. Syst. Nanostruct. 30 (2005) 182.